New high-resolution phonon spectroscopy using impulsive stimulated Brillouin scattering

S. Kinoshita,[a] Y. Shimada, W. Tsurumaki, M. Yamaguchi, and T. Yagi
Research Institute for Electronic Science, Hokkaido University, Sapporo 060, Japan

(Received 9 March 1993; accepted for publication 23 August 1993)

Impulsive stimulated Brillouin scattering is applied to a new high-resolution phonon spectroscopy, where phonons created by two crossing pump pulses are observed using diffraction of a cw probe light in both time and frequency domains. In time domain, real-time behavior can be detected sensitively using a digital oscilloscope, while in frequency domain, measurements with high resolution are attainable by means of a spherical Fabry–Perot interferometer. Several examples of the measurements on liquid samples are demonstrated for clarifying various aspects of the phonon generation by the present method: the mechanism of the generation under pulsed light irradiation, the propagation of the generated phonon, the resonance excitation, and the interference with the other nonlinear optical processes. The relation with the ordinary light scattering is also discussed.

I. INTRODUCTION

Low-frequency phonon spectroscopy has long been attracting much interest. Particularly, in phase transition phenomena, it is often observed that the characteristic frequency of a certain lattice vibration mode gradually decreases, as the temperature approaches the transition point. This mode, called a soft mode, has been the main subject of extensive study for elucidating the mechanism of the structural phase transitions. Optical approach to investigate this soft mode is very convenient, because it is easy to measure without any contact with a sample and gives an extremely local information. Light scattering measurements such as Brillouin scattering and low-frequency Raman scattering are typical methods for this purpose and have been utilized in various ways.

However, when the temperature comes very close to the transition point, the phonon mode softens considerably, i.e., the characteristic frequency of the soft phonon is unlimitedly going to zero. Hence, a very low-frequency phonon spectroscopy is undoubtedly needed. Ordinary light scattering experiment is the frequency-domain measurement and inevitably uses monochromators such as a diffraction grating type or a Fabry–Perot type. On account of the finite resolution of the monochromator, the observation of the low-frequency mode becomes quite difficult particularly near the phase transition point. In fact, if the frequency shift of the low-frequency mode becomes comparable to the frequency resolution, the elastic and quasi-elastic (Rayleigh) components, which broaden on account of the limited resolution, overlap the phonon mode and it is actually impossible to discriminate the spectra of the phonon mode from these components.

Nelson and Fayer[1] developed phonon spectroscopy using impulsive stimulated Brillouin scattering (ISBS). This method is based on the time-domain measurement and is applicable even to the measurement of very low-frequency phonons. They applied this method successfully to various materials such as liquids,[1–3] glasses,[4] crystals,[1,5–9] and thin films.[10] The principle of ISBS is as follows: Consider the case where two coherent light beams having slightly different frequencies are incident into a material. If the frequency of the phonon is equal to their frequency difference, the stimulated emission takes place and the intensity of the light with the lower frequency increases accompanying the generation of phonons. In ISBS, instead of using two frequency-stabilized lasers, a light pulse from a laser is divided into two to make a transient interference fringe in the material and leads to the generation of phonon through the interaction between the light and material. In this case, a pitch of the interference fringe gives a wavelength of the phonon. Furthermore, since the frequency spectrum of the light broadens due to the finite duration of the pulse, the different frequency components of divided pulses work as two frequency-different coherent lights. Thus, the energy and momentum conservations are automatically satisfied. The generated phonons are observed by the diffraction of a probe light. Since the observation of the phonon dynamics is performed in time domain, extremely high resolution in frequency region is attainable.

Recently, Robinson *et al.*[6] applied ISBS to observe the soft acoustic mode in KH_2PO_4 (KDP) near the transition point. Since then, several ferroelectrics such as RbH_2PO_4 (RDP)[7] and tri-sarcosine calcium chloride (TSCC)[8] were studied by this method. In these measurements, the time dependence of the phonon generated by ISBS was measured by diffracting the pulsed light and the time dependence is obtained by scanning an optical delay. In this case, the measurable time range is restricted by the maximum length of the optical delay and the measurement of the soft mode with very low frequency often gets into difficulty. In the present study, we have employed a cw laser as a probe and have constructed a new phonon spectroscopy based on the principle of ISBS (ISBS phonon spectroscopy). Particularly, to employ a cw laser as a probe is excellent because

[a]Present address: Department of Physics, Faculty of Science, Osaka University, Toyonaka, Osaka 560, Japan.

 0034-6748/93/64(12)/3384/10/$6.00

the phonon dynamics are investigated in real time by means of a digital oscilloscope and also the frequency-domain measurement is easily obtainable with a Fabry–Perot interferometer coupled with a cw probe laser operated in a single-frequency mode. In the following, we will show the usefulness of this spectroscopy by demonstrating several features of the generated phonons in liquid samples. A part of the present work has been already reported.[11]

II. PRINCIPLE OF THE ISBS PHONON SPECTROSCOPY

First, we briefly review the principle of phonon generation by light pulses. When a light pulse is incident into a material, the light can be coupled with the elastic strains through photothermal and photoelastic effects. The former comes from the local light absorption followed by the heat release, temperature rise, and then thermal expansion. The latter is originated from the force by the electric field of the light against the polarization which is induced by the thermal fluctuation of the dielectric constant under the electric field of the light.

The state of the material under the external light field is generally expressed by the conservation rules of mass, momentum, and energy. In liquid, these relations become simplified into the following two equations concerning the changes of the density and the temperature, which are well known for stimulated Brillouin scattering.[12]

$$\frac{\partial^2\rho_1}{\partial t^2}-\frac{v^2}{\gamma}\Delta\rho_1-\frac{v^2\beta\rho_0}{\gamma}\Delta T_1-\frac{\eta}{\rho_0}\Delta\frac{\partial\rho_1}{\partial t}=-\frac{\gamma_e}{8\pi}\Delta E^2, \tag{1}$$

$$\rho_0 C_v\frac{\partial T_1}{\partial t}-\lambda\Delta T_1-\frac{C_v(\gamma-1)}{\beta}\frac{\partial\rho_1}{\partial t}=\frac{nc\alpha}{4\pi}E^2, \tag{2}$$

where ρ_1 is the deviation of the density from its average value ρ_0, and T_1 is that of the temperature. v, β, η, and λ are sound velocity, thermal expansion coefficient, viscosity, and heat conductivity, respectively. $\gamma=C_p/C_v$ with the specific heat at constant pressure and volume, C_p and C_v. γ_e is a constant expressing the magnitude of the coupling between light and elastic strain through the photoelastic effect. In liquid, this constant is expressed as n^4p, where n and p are the refractive index and the photoelastic constant. α is the absorption coefficient of the light by the material and c is the light velocity in vacuum. In the above expressions, viscous fluid is assumed and the changes in the local temperature and density are assumed to be sufficiently small. The right hand sides of Eqs. (1) and (2) express that the light and material couple through the photoelastic and photothermal effects, respectively. E is the sum of the electric fields of the light pulses and is expressed as

$$E=\sum_{j=1}^{2}E_j(t-\tau_j)\exp\{i[\mathbf{k}_j\cdot\mathbf{r}-\omega_1(t-\tau_j)]\}+\text{c.c.}, \tag{3}$$

where two light pulses delayed by τ_1 and τ_2 are assumed to have the same angular frequency ω_1, but have different wave vectors, $\mathbf{k}_1$ and $\mathbf{k}_2$. These two pulses cross in the material with an angle of θ, as shown in Fig. 1. Inserting Eq. (3) into Eqs. (1) and (2), and solving these equations, we obtain the induced dielectric constant $\delta\epsilon(\mathbf{r},t)$ as

$$\delta\epsilon(\mathbf{r},t)=\{n^4K_B^2p/(4\pi\omega_b\rho_0)\}\exp(i\mathbf{K}_B\cdot\mathbf{r})\times\int_{-\infty}^{t}dt'\,L(t-t')E_1(t'-\tau_1)E_2^*(t'-\tau_2), \tag{4}$$

where $L(t)$ is a response function and is expressed as

$$L(t)=-\gamma_a[\exp(-\tfrac{1}{2}\Gamma_R t)-\exp(-\tfrac{1}{2}\Gamma_B t)\cos(\omega_b t)]+\gamma_e\exp(-\tfrac{1}{2}\Gamma_B t)\sin(\omega_b t). \tag{5}$$

Here, $\omega_b=(\omega_B^2-\Gamma_B^2/4)^{1/2}$, and $\mathbf{K}_B=\mathbf{k}_1-\mathbf{k}_2$ with $K_B=2k_1\sin(\theta/2)$. ω_B and Γ_B are the angular frequency and damping constant of the generated phonon. γ_a expresses the contribution of the photothermal effect to the dielectric change and is expressed as $\gamma_a=2nc\alpha v^2\beta/(C_p\omega_b)$. The first and second terms of Eq. (5) correspond to the photothermal and photoelastic contributions. The photothermal term is characterized by the coexistence of the relaxational term and the damped harmonic oscillation. The relaxational term, whose rate Γ_R is expressed by $\Gamma_R=2\lambda K_B^2/\rho_0C_v$, indicates that the spatially periodic temperature distribution, i.e., thermal grating, remains after the propagation of the phonon and then becomes obscure by the heat diffusion. Since the phonon generation through the photothermal mechanism is always accompanied by the thermal grating and also the decay rate of the thermal grating is generally small compared with that of the phonon, $\delta\epsilon(\mathbf{r},t)$ does not alter the sign during the phonon oscillation. On the other hand, $\delta\epsilon(\mathbf{r},t)$ connected with the photoelastic process alters the sign with the phonon oscillation.

When the third pulse delayed by τ_3, electric field of which is expressed by

$$E_3(t-\tau_3)\exp\{i[\mathbf{k}_3\cdot\mathbf{r}-\omega_3(t-\tau_3)]\}+\text{c.c.}$$

is incident to the excitation region, the following polarization is induced through the dielectric change caused by the two preceding pulses:

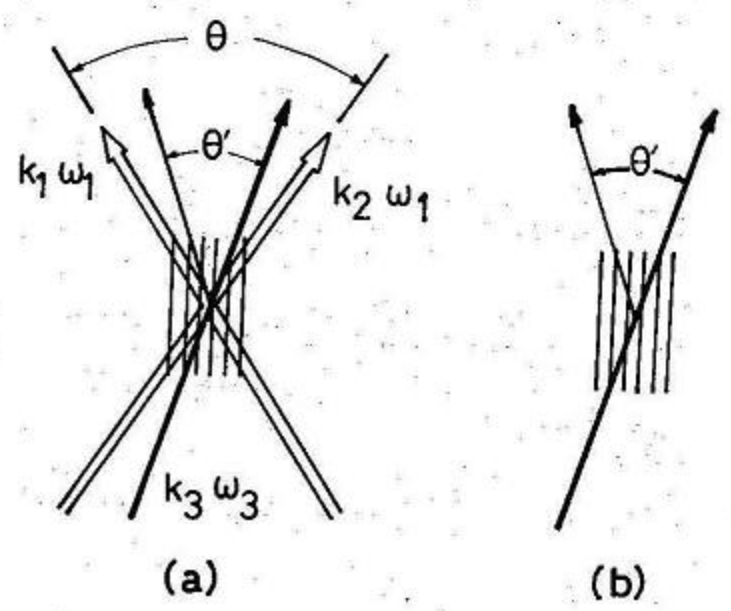

FIG. 1. Schematic diagrams for (a) ISBS phonon spectroscopy and (b) ordinary light scattering experiment. θ expresses the crossing angle of the pump pulses, while θ' the scattering angle of the probe light. Longitudinal lines indicate the wave fronts of the (a) light-induced and (b) thermal phonons.

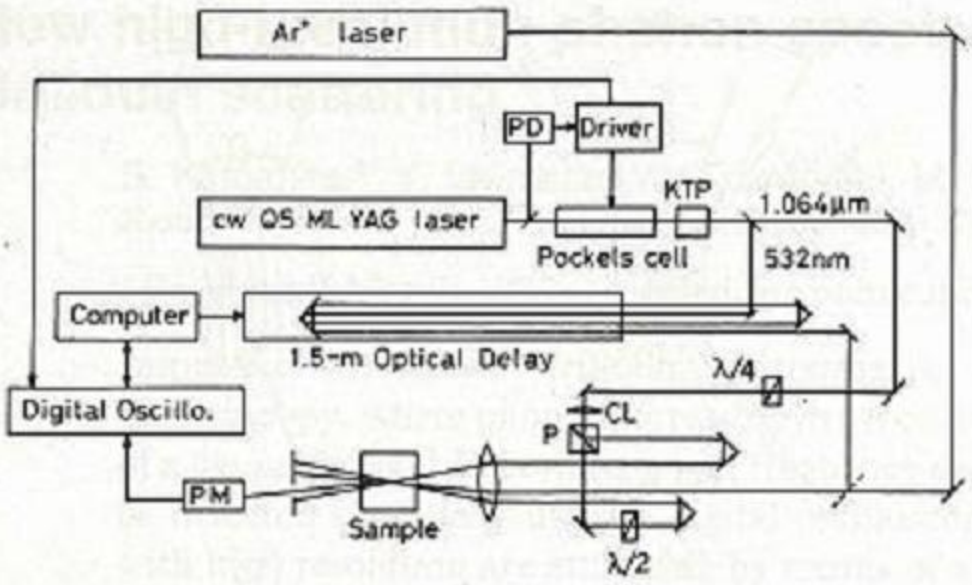

FIG. 2. Block diagram of the ISBS phonon spectroscopy. PD, photodiode; PM, photodetector; Digital Oscillo., digital oscilloscope; P, beam-splitting Glan-laser polarizer; and CL, cylindrical lens.

$$P(\mathbf{r},t)=\exp[i(\mathbf{k}\cdot\mathbf{r}-\omega_3 t+\phi)]\delta\epsilon(\mathbf{r},t)E_3(t-\tau_3)+\text{c.c.} \quad (6)$$

Here, $\mathbf{k}=\mathbf{k}_1-\mathbf{k}_2+\mathbf{k}_3$ and ϕ is a phase factor coming from the variations of the arrival times of the three pulses. The light intensity observed in the direction of the wave vector κ is expressed as

$$I_d(\tau_3)\propto\int dt\left\langle\left|\int d\mathbf{r}\,P(\mathbf{r},t)e^{-i\kappa\cdot\mathbf{r}}\right|^2\right\rangle, \quad (7)$$

where $\langle\cdots\rangle$ means the ensemble average for the electric fields of the light pulses. Then the diffracted light intensity is proportional to the square of the dielectric change. Hence, in case of the photothermal mechanism, the intensity of the diffracted light oscillates at the same frequency as the phonon, while in case of the photoelastic mechanism, the observed frequency of the oscillation is twice the phonon frequency.[1]

III. EXPERIMENTAL PROCEDURE

The block diagram of our apparatus is shown in Fig. 2. The major part of the system is similar to that reported recently.[13] As a light source, a cw mode-locked Nd:YAG laser (NEC, model SL115L) was operated in Q-switching mode with the repetition rate of 100 Hz. The output of the laser formed a pulse train consisting of ~20 mode-locked pulses whose repetition rate was 160 MHz. The pulse width was ~300 ps with the peak power of ~160 kW. The output of the laser was introduced into a Pockels cell (Quantum Technology, model 301-27) to select a single pulse from the mode-locked pulse train and was passed through a KTP ($KTiOPO_4$) crystal for the second-harmonic (SH) generation. The infrared (IR) light pulse (1.064 μm) was separated from the SH pulse (532 nm) by a dichroic mirror and was used for exciting the phonon, while the SH pulse was used as a probe. For the selective excitation of phonon, we employed a pulse train instead of a single pulse.

The IR pulse was circularly polarized by a $\lambda/4$ plate, and then fed into a beam-splitting Glan-laser prism (Karl Lambrecht). The two pulses divided by this prism have polarizations vertical (V) and horizontal (H) to an optical table, respectively. Furthermore, a $\lambda/2$ plate was inserted into the optical path for one of the divided pulses. This provided an easy selection for the VV, VH, and HH excitation. The two IR pulses were led into two optical delays to adjust the timing of the two pulses, made parallel to each other, and then focused into a sample through a lens with large aperture. The two IR pulses formed an interference fringe by their electric fields. This causes the generation of two counterpropagating phonons at the focal region through the interaction with the material as described in the preceding section. The wavelength of the phonon generated is expressed as $\Lambda=\lambda_1/2\sin(\theta/2)$, with the crossing angle θ and the wavelength of the light λ_1. The third light pulse, a probe, was then incident to the focal region so as to make a Bragg angle to the interference fringe. The diffracted light was then detected by a photodetector such as a photomultiplier or a photodiode. The intensity of the diffracted light oscillated according to the propagation of the phonons which existed as a standing wave. Since the generated phonon is expressed as a wave packet whose geometry is determined by the excitation region, it flees from the detection region on account of the propagation. To avoid this effect, a cylindrical lens with a focal length of 0.5 m was inserted into the optical path. This made a flat plate-like focal region with the maximum length of ~0.6 mm across the interference fringe.

Unlike recent measurements, we employed a cw Ar^+ laser (Lexel, model 95) as a probe. The time dependence of the diffracted light was obtained by directly feeding the output of the photodetector to a 500 MHz digital oscilloscope (Sony Tektronix, model TDS540). This method is excellent because the complete time dependence of the diffracted light intensity is recorded for every exciting pulse. This enables a real-time measurement and also saves the acquisition time. Furthermore, to employ the cw laser enables us to perform easily the frequency-domain measurement without changing the experimental configuration. To do this, the Ar^+ laser was operated in a single-frequency mode, and a spherical Fabry–Perot interferometer (Spectra Physics, model 470-01) was inserted between the photodetector and the sample. The output of the photodetector was fed into a Boxcar averager (EG&G PAR, model 4121B) whose gate width was adjusted so that only the oscillatory signal due to the generated phonon was averaged. The outputs of the digital oscilloscope and the Boxcar averager were transferred into a personal computer for the data analysis. We also employed the SH pulse as a probe. In this case, the diffracted light was detected by the photodetector and its output was fed into the Boxcar averager and transferred to the personal computer. The time dependence of the diffracted light intensity was obtained by scanning a large optical delay under a computer control.

Compared to the method reported previously, it has the advantage of employing a cw laser as a probe because the measurable time range extends actually to the infinite and hence is particularly suitable for the measurement of slow dynamics in the phase transition. Eichler and Stahl[14] first attempted the cw probing for phonons induced through the photothermal process of a Q-switched, mode-locked ruby laser and successfully demonstrated the obser-

vation of the phonon dynamics. However, their data were collected only for the pulse train excitation and also the obtained data were not so clear possibly because of the poor laser stability and detection sensitivity at that time. Our method of cw probing has opened a new field to the low-frequency phonon spectroscopy by introducing a real-time time-domain measurement and also a high-resolution frequency-domain measurement. Particularly, the frequency-domain measurement utilizing ISBS has been done for the first time in the present work. Furthermore, combining the frequency-domain measurement with ISBS is superior for detecting weak signals, since in ordinary time-domain measurement there is no spectral exclusion of scattered probe light which appears as the unwanted background noise.

To measure the fast response, however, the cw probing has a limit in its time resolution. The time resolution of our system is determined by the response time of the photodetector and the oscilloscope. Furthermore, a low instantaneous intensity of the cw light gives a poor signal-to-noise ratio. To employ the SH pulse as a probe is advantageous in this sense because the time resolution of the system is determined only by the width of the pulse employed and also because of the high instantaneous intensity. However, in this case the observable time range is a weak point. For example, in our case, the maximum delay time of 20 ns is obtainable by double passing the 1.5 m optical delay. Therefore the combination of these two kinds of the probe is practically suitable for covering a wide observable time range.

Nelson and Fayer[1] used one more Pockels cell to select a mode-locked pulse from the pulse train one after the other and covered the wide time range by combining an optical delay. Duggal and Nelson[3] also employed one more cw mode-locked, Q-switched Nd:YAG laser solely for the generation of the probe pulse. This allows the measurement in the infinitely wide time range without loss of the probe intensity. They also attempted a broad Q-switched Nd:YAG laser as a probe and used a transient recorder as the data accumulation.[10] This method allows a real-time measurement, but the nonuniform intensity profile of the probe pulse may obscure the data. Our method to combine the cw laser with the digital oscilloscope is simple, but is very effective, because the infinitely wide time range is covered at once by the real-time measurement, which extremely shortens the measuring time. In fact, the time-domain measurements shown in the subsequent section were made within only 3 s after averaging 300 records. In the following, we will demonstrate the usefulness of the present ISBS phonon spectroscopy by showing the various features of the phonon generation.

IV. EXPERIMENTAL RESULTS

A. Photothermal and photoelastic mechanisms for phonon generation

We first show the essential features of the phonon generation (in the present case, acoustic wave generation) by light pulses using liquids as an isotropic sample. In Fig. 3,

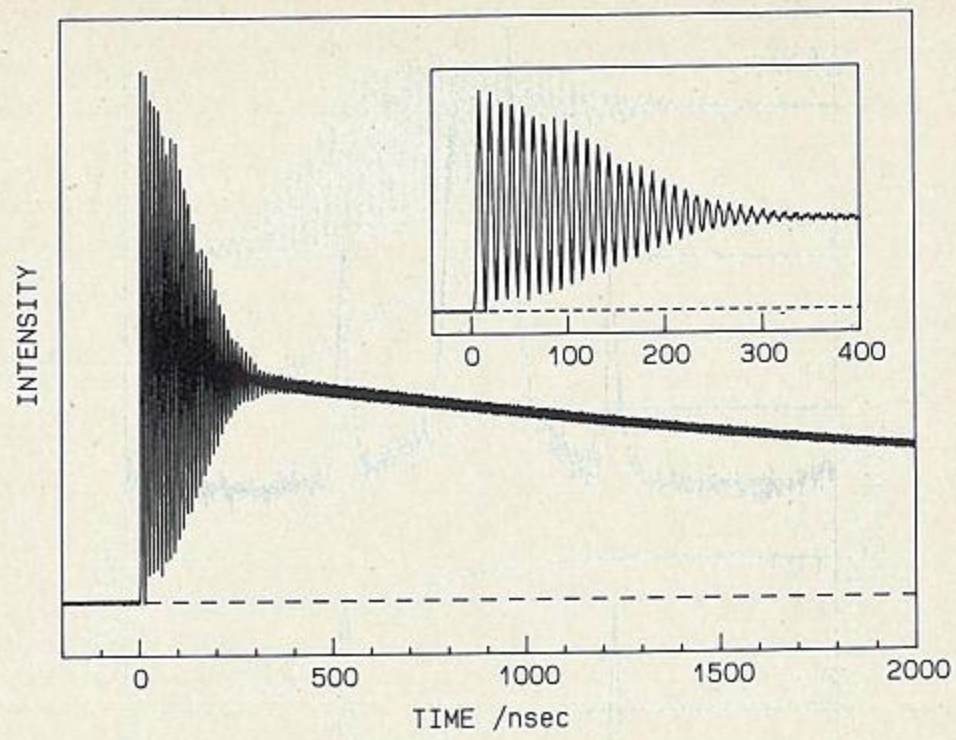

FIG. 3. Typical example of the time response of the acoustic mode generated by the present method through photothermal effect. Sample is ethanol.

we show the typical result on ethanol at room temperature. The time dependence consists of an oscillatory signal with the frequency of ~ 80 MHz and a slowly decaying component with the decay time of $\sim 4\ \mu$s. The former comes from the acoustic waves in a standing wave, while the latter from the thermal grating. The damping observed in the oscillatory signal is related to the damping of the acoustic waves themselves and also to the propagation of the wave packets from the detection region. From the analysis of the observed number of the interference fringe, the latter effect is found more dominant in this experiment. Thus, we should pay attention to the extent of the excitation region to measure accurately the frequency and damping of the generated phonon when it has a very low frequency. On the other hand, the damping found in the thermal grating is originated solely from the heat diffusion. The feature of these time dependences are characteristic to the case the phonon is generated through the photothermal effect.

The phonon generation through the photoelastic effect shows a somewhat different result. In Fig. 4, the result on

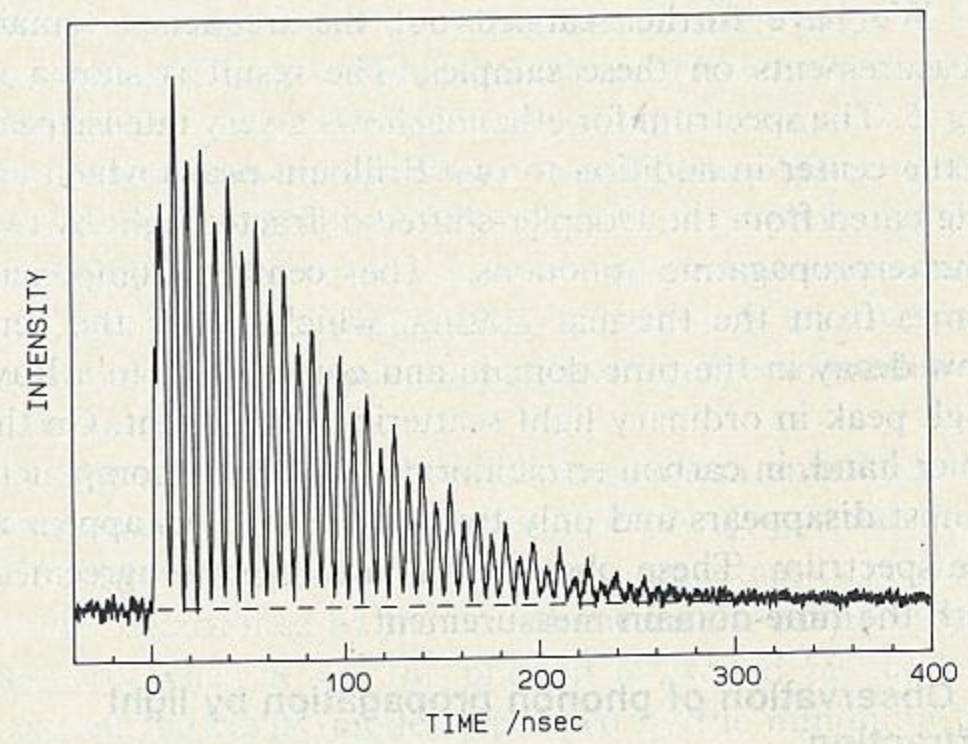

FIG. 4. Typical example of the time response of the acoustic wave generated by the present method through photoelastic effect. Sample is carbon tetrachloride.

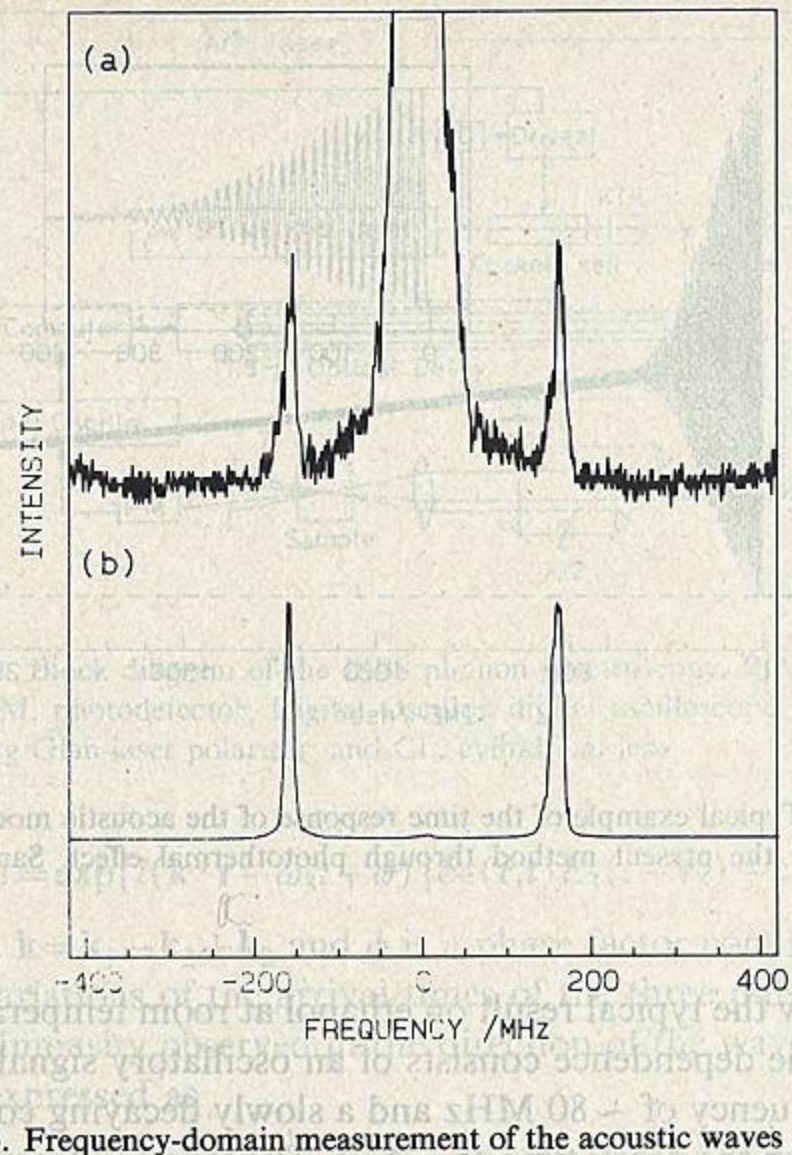

FIG. 5. Frequency-domain measurement of the acoustic waves generated by the present method through (a) photothermal (ethanol) and (b) photoelastic (carbon tetrachloride) effects.

carbon tetrachloride is shown. It is easily noticed that a slowly decaying component found in ethanol does not appear in this case. Furthermore, the frequency of the oscillatory signal is twice the acoustic frequency calculated from the sound velocity. As mentioned above, these features are characteristic to the case that the phonon is generated through the photoelastic effect. The small alternative intensity variation found in Fig. 4 comes from the interference with a small amount of the stray light due to the scattered probe light at the surface of the sample cell. We measured the time dependence for various liquids and found that the photothermal effect is prominent for liquids having hydrogen atoms within a molecular structure. This may be because the third overtone ($\sim$9000 cm^{-1}) of hydrogen stretching mode is close to the energy of the IR pulse of 9394 cm^{-1}.

We have further carried out the frequency-domain measurements on these samples. The result is shown in Fig. 5. The spectrum for ethanol shows a very intense peak in the center in addition to two Brillouin peaks which are originated from the Doppler-shifted diffracted light by two counterpropagating phonons. The central component comes from the thermal grating, which shows the very slow decay in the time domain and corresponds to a Rayleigh peak in ordinary light scattering experiment. On the other hand, in carbon tetrachloride the central component almost disappears and only two Brillouin peaks appear in the spectrum. These observations are in good agreement with the time-domain measurement.

B. Observation of phonon propagation by light diffraction

Acoustic waves generated through either photothermal or photoelastic process propagate as a wave packet from

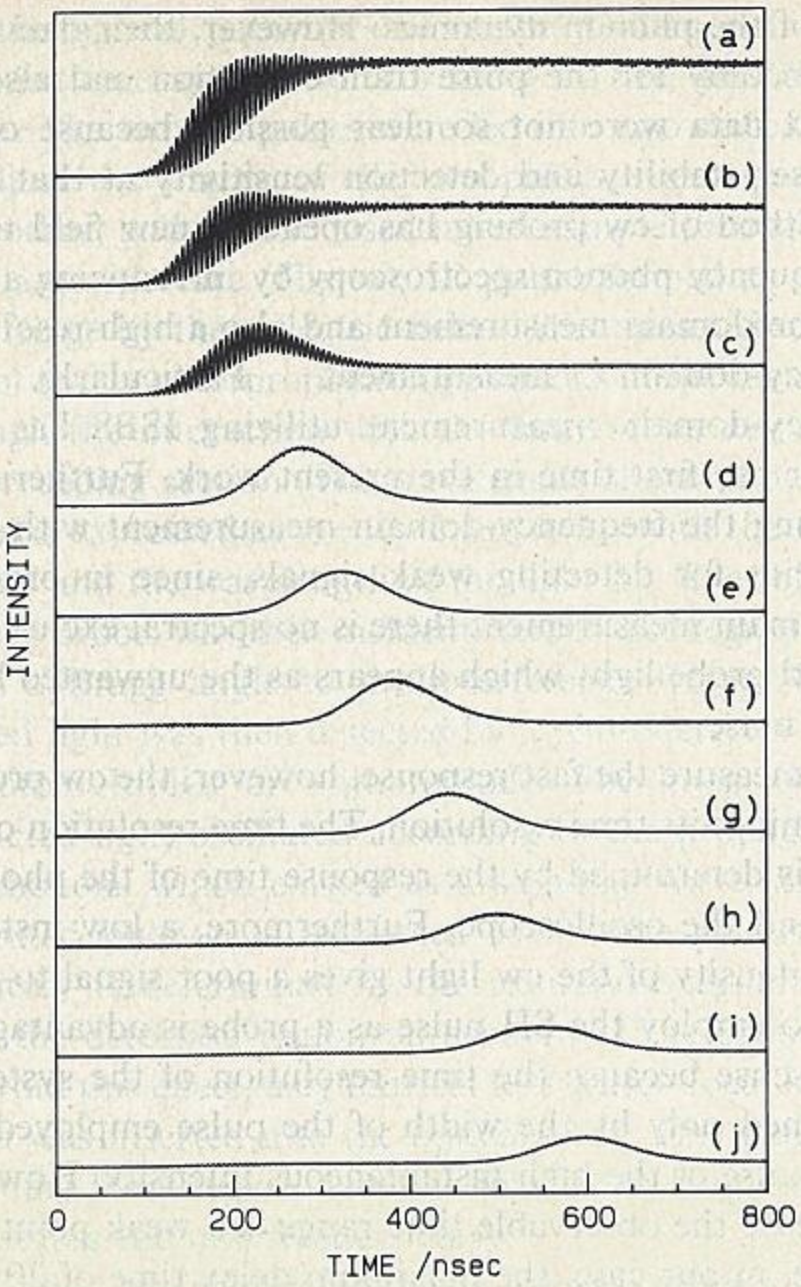

FIG. 6. Time dependence of the probe light intensity diffracted from acoustic waves generated by ISBS in ethanol. The positions of the probe light are (a) 0, (b) 0.06, (c) 0.12, (d) 0.19, (e) 0.25, (f) 0.31, (g) 0.37, (h) 0.44, (i) 0.50, and (j) 0.56 mm separated from the excitation region.

the excitation region. We can observe the propagation of the acoustic waves by the diffraction of a probe light. To do this, a small glass plate with a thickness of 5 mm was inserted into the optical path of the probe beam just after the focusing lens and was rotated so as to slightly change the detection region without changing the Bragg angle. In Fig. 6, we show the result on ethanol in the time domain. When the probe light is passing through the excitation region, the phonon oscillation and the slowly decaying component are observed as in Fig. 3. As the probe light deviates from the excitation region, both the oscillation and the slowly decaying component gradually disappear and the diffracted light is observed after some time delay from the excitation pulse. This indicates that the probe light is passing through the place where only a traveling acoustic wave exists and that the time delay is due to the finite velocity of the acoustic wave. In fact, the time delay and the deviation of the detection position from the excitation region give the sound velocity of the sample with good experimental accuracy. Thus the direct observation of the phonon propagation has been accomplished for the ISBS-induced phonons. The similar time-domain experiment has not been attempted since the earlier experiment done by the above-mentioned authors,[14] though reports on the acoustic waves excited by transducers have appeared occasionally.[15]

On the other hand, in the frequency domain, the above

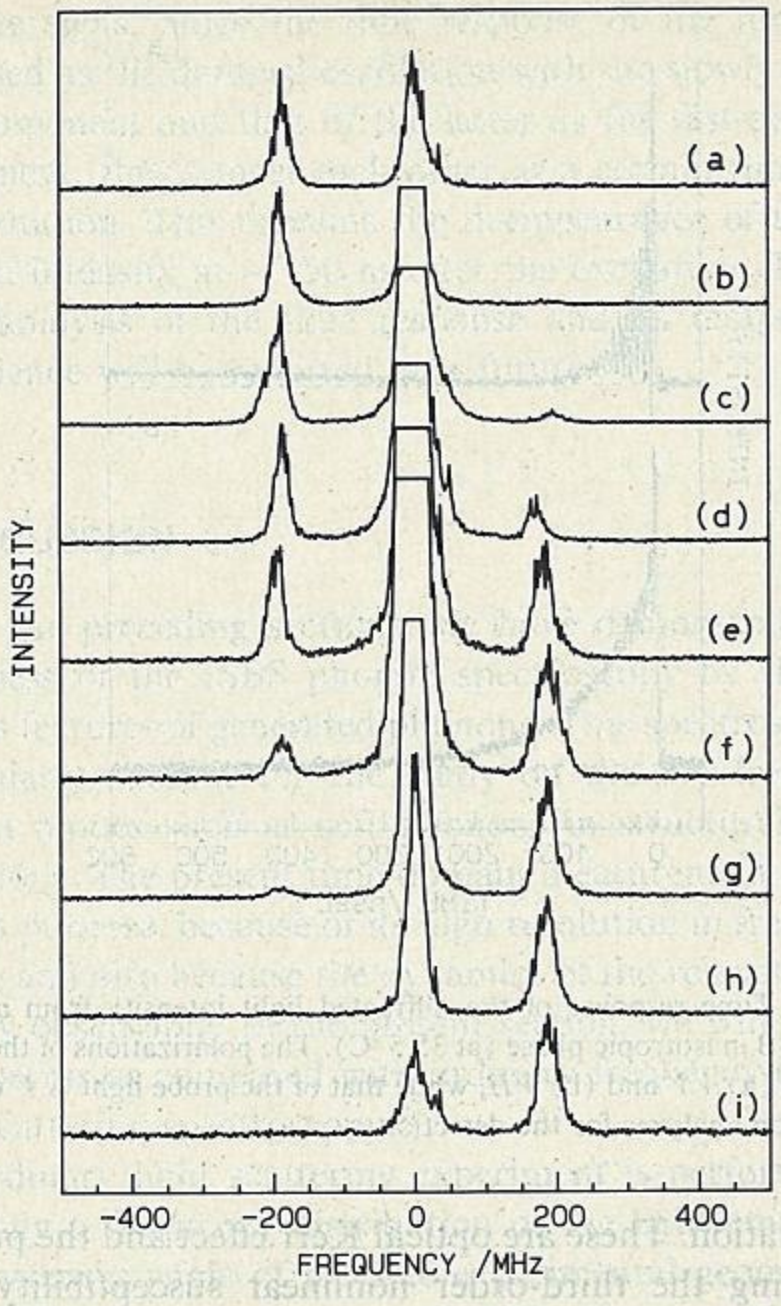

FIG. 7. Frequency-domain measurements of the acoustic wave generated by ISBS in ethanol. The probe position is varied as mentioned in the literature. The positions of the probe beam are (a) −0.10, (b) −0.07, (c) −0.05, (d) −0.02, (e) 0, (f) 0.02, (g) 0.05, (h) 0.07, (i) 0.10 mm separated from the excitation region. Notice that two Brillouin peaks are observed in the excitation region, while only one peak is observed in the area where only a traveling phonon exists.

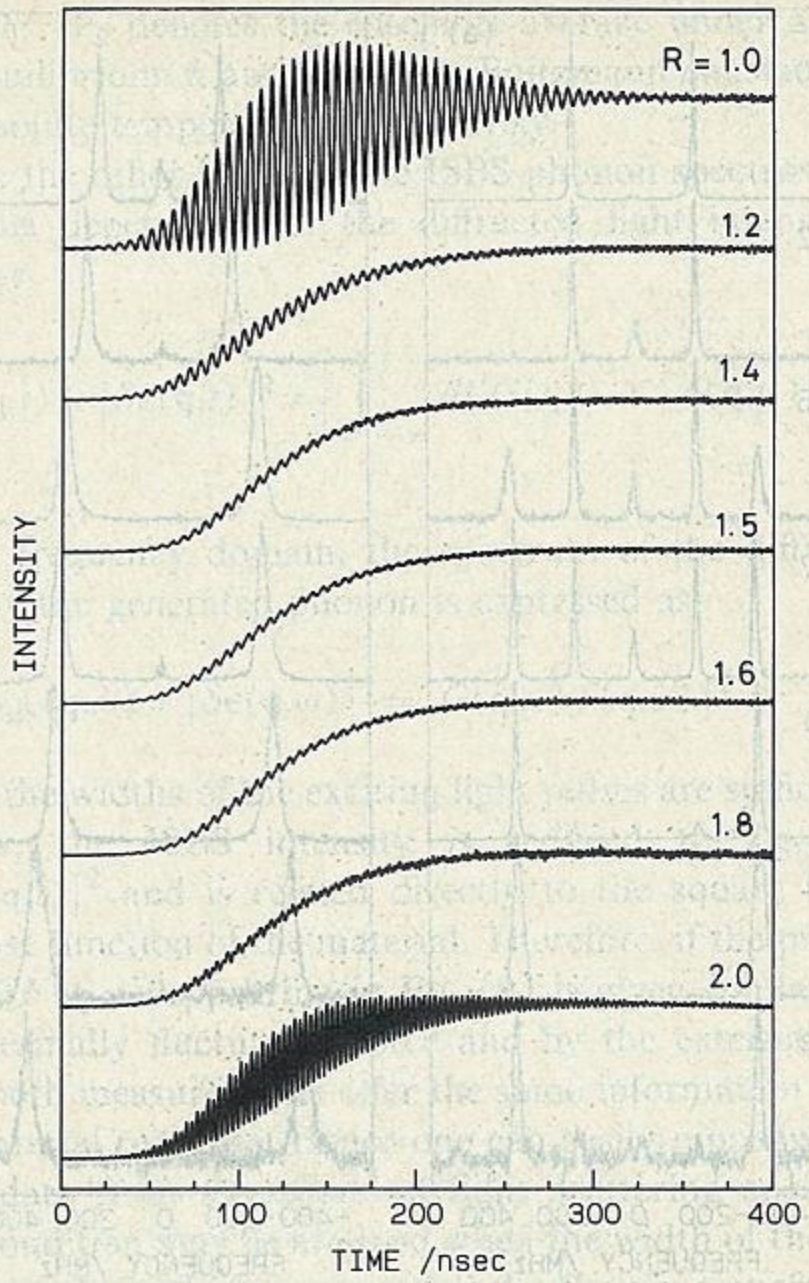

FIG. 8. Resonance effect of the ISBS phonon generation in ethanol using a pulse train for the various ratios R of the pulse repetition rate to the phonon frequency determined by the crossing angle of the pump pulses. Sample employed was ethanol. Notice at $R=1$ and 2 the phonon amplitude is resonantly enhanced.

observation appears more remarkable as the difference of the spectrum. Namely, as shown in Fig. 7, in the excitation region, the spectrum usually shows a strong Rayleigh peak and two Brillouin peaks located at both sides of the Rayleigh peak corresponding to the Stokes and anti-Stokes lines. When the probe light is far from the excitation region, only a single Brillouin peak at either side is alive and at the same time the intensity of the Rayleigh peak decreases.

C. Resonance excitation of phonon by repetitive pulse train

In the above measurements, we did not care whether the excitation was done by a single pulse or by a pulse train. However, interesting phenomenon occurs when the pulse train is employed as the excitation. We first show the time-domain measurement in Fig. 8. In this experiment, we change the crossing angle of the two exciting pulses so that the relation between the repetition rate of the exciting pulses and the phonon frequency determined by the crossing angle is adjustable. In this figure, the ratio R of the latter to the former is varied from 1.0 to 2.0. The sample employed is ethanol. It is found that at $R=1.0$, the amplitude of the oscillation due to the generated phonon is found to increase resonantly. The diffraction due to the thermal grating also increases with time. This is because under periodic excitation the forced oscillation takes place in the resonance condition. Namely, when R becomes close to unity, the amplitude of the phonon generated by the preceding pulse adds in phase to that generated by the present pulse and the amplitude of the phonon is resonantly increased. On the other hand, around $R=1.5$, the phonon generated by one pulse destructively adds to the preceding one, and hence almost no phonon is excited. Even in this case, the thermal grating is accumulated because of its slow decay. When $R=2.0$, the phonon generated by one pulse is alternately added in phase to that generated by the preceding pulse, therefore the resonant enhancement takes place again. In this case, however, the amplitude of the phonon is increased every two oscillatory periods.

The time characteristics of the phonon amplitude are determined by the intensity profile of the Q-switched light pulse. In the mode-locked condition, the intensity profile is further determined by the beats between the cavity modes. Namely, when $R=1$, the phonon is excited by the beat between the cavity modes separated by the minimum frequency difference. When $R=2$, the time characteristics are explained by the beat between the cavity modes which have twice the minimum frequency difference. In the intermedi-

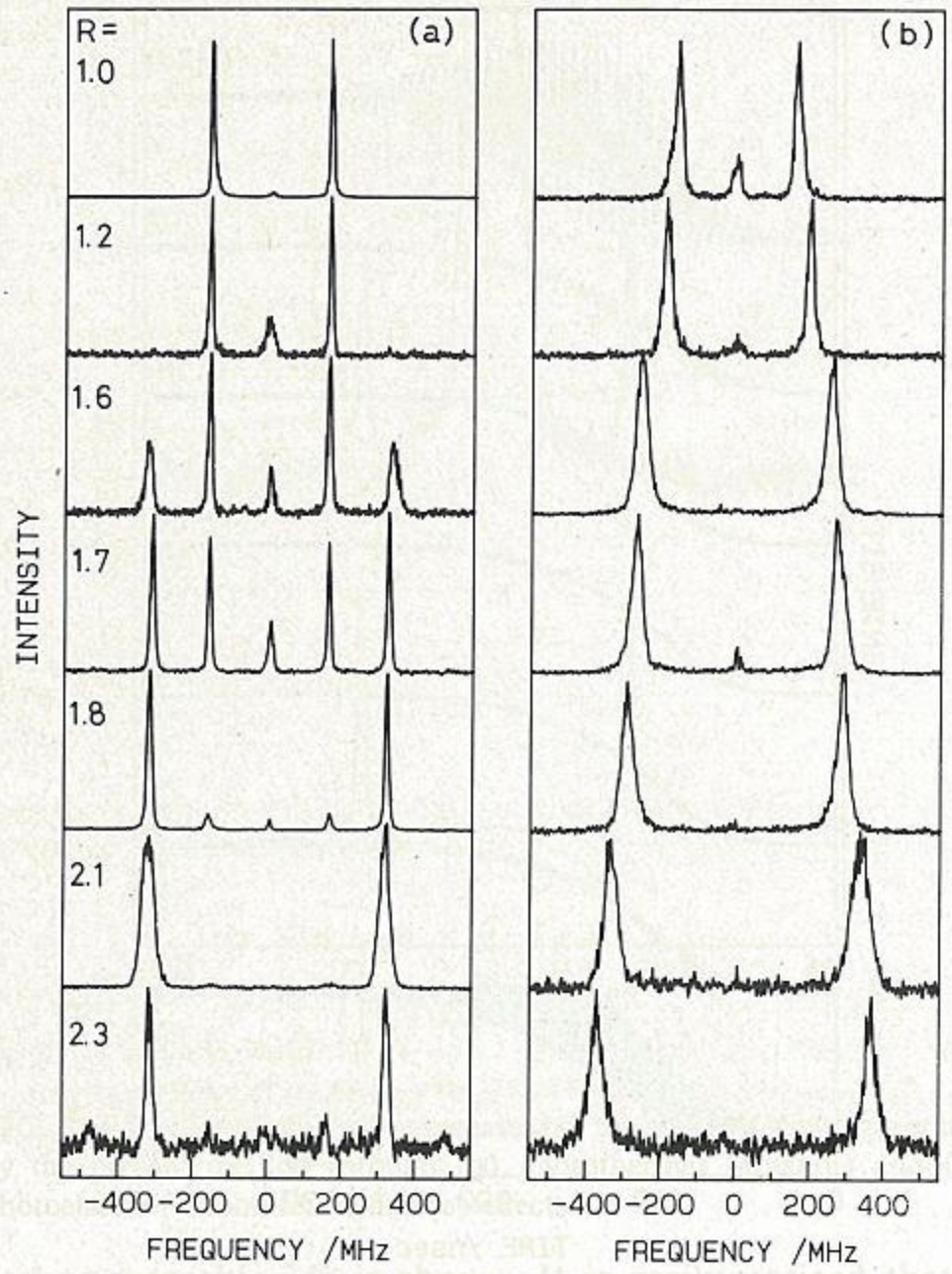

FIG. 9. Frequency-domain measurement on the resonance effect of the ISBS phonon generation in carbon tetrachloride. (a) A pulse train and (b) a single pulse are employed as an excitation for various values of the ratio R.

ate case between $R=1$ and 2, they should be expressed by the superposition of the above two cases. In fact, as shown in Fig. 9(a), the frequency-domain measurement on carbon tetrachloride shows that the spectrum consists of a Brillouin doublet near the resonant case, i.e., with the frequency shift of 160 MHz for $R=1$, which is the minimum frequency difference of our laser modes, and 320 MHz for $R=\sim 2$. On the other hand, in the intermediate case, two Brillouin peaks definitely appear both in the Stokes and anti-Stokes sides and the intensity ratio of the two varies with R. The dependence of this intensity ratio on R is determined by the intensity profile of the exciting pulse train. This result is in contrast with that obtained under a single-pulse excitation, where a Brillouin peak merely shifts according to the crossing angle of the pump pulses [Fig. 9(b)].

Although the use of the pulse train to excite the phonon has been demonstrated frequently in various experimental configurations,[1,14,16,17] this work, for the first time, has clarified the spectrum of the phonon excited by repetitive pulses through ISBS. This technique may be useful for the detection of the weak phonon mode buried in the broad nonoscillating mode.

D. Interference between the phonon generation and the other nonlinear optical processes

In the ISBS phonon spectroscopy, various nonlinear optical processes take place under the same experimental

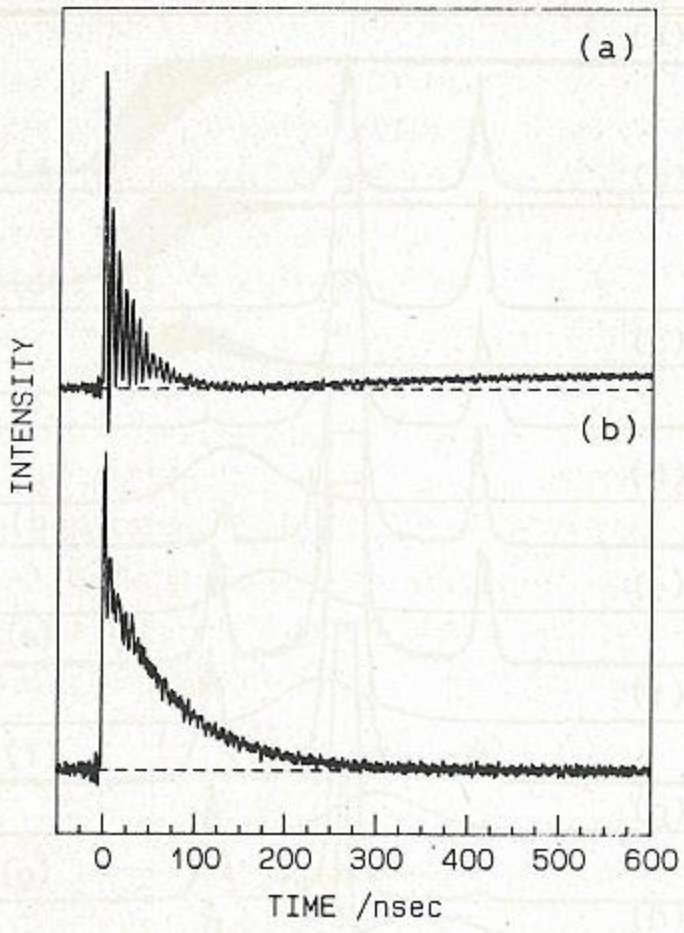

FIG. 10. Time response of the diffracted light intensity from a liquid crystal 5CB in isotropic phase (at 35.5 °C). The polarizations of the pump pulses are (a) VV and (b) VH, while that of the probe light is V without polarization analyzer for the detection.

configuration. These are optical Kerr effect and the process concerning the third-order nonlinear susceptibility. Recently, we have reported[13] that these processes add extra terms to the induced polarization for the acoustic wave generation of Eq. (5). Since the observed time response is proportional to the square of the induced polarization, the interference effect appears in the time dependence of the diffracted light intensity. For example, in carbon tetrachloride, these processes appear as a sharp component around a time origin and under repetitive excitation this component appears as a peak or a dip according to the phase of the phonon oscillation. In carbon disulfide, well known as a Kerr medium, shows a more prominent time dependence. Namely, a sharp peak and a broad component, which are connected with the coherent and incoherent couplings between the pump and probe pulses, overlap the ordinary phonon oscillation and deform the time response.

In order to investigate further this interference effect, we have chosen the isotropic phase of a liquid crystal as a sample,[18,19] because liquid crystals are known to show slow relaxations in the optical Kerr response.[20] The results on 5CB (p-n-pentyl-p'-cyanobiphenyl) for the VV and VH excitations are shown in Fig. 10. In the VV excitation, it is shown that the oscillatory signal is accompanied by the background which is once going to zero and again coming back to a nearly constant value. In the VH excitation, the time response is found to decay very fast initially and then decay slowly afterwards. Since the phonon generation in ordinary liquids takes place only under the VV excitation, the time response for the VH excitation can be ascribed mainly to the optical Kerr effect. Comparing the results for the two polarization geometries, the time response for the VV excitation is explained in terms that both the phonon generation due to the photothermal effect and the optical Kerr effect contribute to the dielectric change, but with

opposite signs. Since the time response of the former is expressed as the damped oscillation with the slowly decaying component and that of the latter as the fast-decaying component, they cancel each other at a certain time after the excitation. This explains the disappearance of the diffraction intensity at ~150 ns after the excitation. The detailed analysis of the time response and its temperature dependence will be reported near future.

V. DISCUSSION

In the preceding sections, we have demonstrated the usefulness of the ISBS phonon spectroscopy by showing various features of generated phonons. This spectroscopy is particularly suitable for the study on the low-frequency phonon modes such as soft phonons in structural phase transitions. The present time-domain measurement is ideal for this purpose, because of its high resolution in frequency region, and also because the dynamics of the relaxation are directly observable. In the present section, we will discuss these points as compared with ordinary frequency-domain light scattering spectroscopy.[21]

Ordinary light scattering experiment is performed by analyzing a frequency distribution of the light emitted at the scattering angle of θ'. The experimental geometry of the ISBS phonon spectroscopy is the same as the light scattering experiment, as shown in Fig. 1. The difference is that in the former thermal phonons are detected in the frequency domain, while in the latter the measurement is done for the light-induced nonequilibrium phonons either in the time or frequency domain. Usually, the dielectric constant of the material fluctuates spatially and temporally under the influence of the thermally induced strain or thermal density fluctuations. Further, the dielectric constant changes under the application of strong light pulses. We put these changes in the dielectric constant as $\delta\epsilon(\mathbf{q},t)$ for the wave vector $\mathbf{q}$ and time t and the force to induce the fluctuation or the change as $F(\mathbf{q},t)$. Then, the following relation holds within a linear response theory:

$$\delta\epsilon(\mathbf{q},t)=\int_{-\infty}^{t} dt' G(\mathbf{q},t-t')F(\mathbf{q},t'), \tag{8}$$

or its Fourier transform

$$\delta\epsilon(\mathbf{q},\omega)=G(\mathbf{q},\omega)F(\mathbf{q},\omega), \tag{9}$$

where $G(\mathbf{q},t)$ is the response function. The force can be divided into two as $F(\mathbf{q},t)=R(\mathbf{q},t)+f(\mathbf{q},t)$, where $R(\mathbf{q},t)$ and $f(\mathbf{q},t)$ are the thermally fluctuating force and the external force by light pulses. $f(\mathbf{q},t)$ is expressed as in the form of $f(\mathbf{q},t)\propto E_1(t)E_2^*(t)\exp(i\mathbf{q}\cdot\mathbf{r})$. In the ordinary light scattering experiment, $f(\mathbf{q},t)=0$, while $R(\mathbf{q},t)$ is negligible in the ISBS phonon spectroscopy.

The ordinary light scattering spectrum $I_{\mathrm{LS}}(\mathbf{q},\omega)$ is obtained through the fluctuation-dissipation theorem as

$$I_{\mathrm{LS}}(\mathbf{q},\omega)\propto\int dt\exp(i\omega t)\langle\delta\epsilon(\mathbf{q},0)\delta\epsilon(\mathbf{q},t)\rangle_R$$
$$\propto(kT/\omega)\mathrm{Im}[G(\mathbf{q},\omega)]. \tag{10}$$

Here, $\langle\cdots\rangle_R$ denotes the ensemble average under a thermal equilibrium. k and T are the Boltzmann constant and the absolute temperature, respectively.

On the other hand, in the ISBS phonon spectroscopy, the time dependence of the diffracted light intensity is given as

$$I_{\mathrm{ISBS}}(\mathbf{q},t)\propto|\delta\epsilon(\mathbf{q},t)|^2=\left|\int_{-\infty}^{t} dt' G(\mathbf{q},t-t')f(\mathbf{q},t')\right|^2. \tag{11}$$

In the frequency domain, the spectrum of the diffracted light by the generated phonon is expressed as

$$I_{\mathrm{ISBS}}(\mathbf{q},\omega)\propto|\delta\epsilon(\mathbf{q},\omega)|^2=|G(\mathbf{q},\omega)f(\mathbf{q},\omega)|^2. \tag{12}$$

When the widths of the exciting light pulses are sufficiently narrow, the ISBS intensity is reduced to $I_{\mathrm{ISBS}}(\mathbf{q},t)\propto|G(\mathbf{q},t)|^2$ and is related directly to the square of the response function of the material. Therefore, if the product $G(\mathbf{q},\omega)F(\mathbf{q},\omega)$ appearing in Eq. (9) is given similarly by the thermally fluctuating force and by the external light field, both measurements offer the same information about the material response. Hence one can easily reproduce the ISBS data from the observed light scattering spectrum. This condition may be attained when the width of the light pulse is sufficiently narrow so that the Fourier transform of the intensity profile for the light pulse covers the frequency region of interest.

However, even in a very low-frequency region, various degrees of freedom such as acoustic waves, the fluctuation of local temperature, and molecular reorientation, overlap in the spectrum. The coupling constants of light with these degrees of freedom through photoelastic constant, absorption coefficient of light, optical Kerr constant, are dependent on the material. Hence the light-induced changes in these degrees of freedom are expected to essentially differ from the thermally activated fluctuations. This may cause the different time behavior of the ISBS response from that calculated from the ordinary light scattering spectrum. Furthermore, if the time width of the pump pulse is not so narrow or the Fourier transform of the intensity profile of the light pulse is not uniform, this difference is more pronounced. Particularly, when the Fourier transform of the light pulse has a sharp peak, the material response which has a component at that frequency may be selectively excited. If we utilize the difference between the ordinary light scattering experiment and the ISBS phonon spectroscopy, it is possible to discriminate the phonon components which overlap spectrally with each other and also to investigate the broadening mechanism of the phonon spectrum. The above feature is clearly understood even in the present experiment. As shown in Fig. 5, the Brillouin spectrum obtained for carbon tetrachloride shows only a negligible amount of the Rayleigh component, whereas the intensity ratio of the Rayleigh to Brillouin component in the ordinary light scattering spectrum is generally given by Landau–Placzek ratio.[22]

Next, we focus our attention to the experimental standpoints. The ISBS phonon spectroscopy consists of

two optical processes: One is the phonon generation by the two light pulses, and the other is the diffraction of the probe light by the phonon. These two processes are essentially the same with each other with respect to the light and material interaction, and are also the same as the ordinary light scattering process. Hence, the wave vector $\mathbf{q}$ of the phonon created and observed by the light pulse is restricted within a region of $|\mathbf{q}| \leqslant \pi/\lambda$, as is usually the case for the ordinary light scattering measurement. However, the most prominent point of the present spectroscopy is located at the fact that coherent phonons are actually generated by light pulses. Namely, under the application of strong light pulses, the vibrations of the generated phonons with definite wave numbers (and hence the electric field of the scattered light by the phonon) oscillate in phase. This yields the light scattering of high intensity and high directionality. These characteristics are particularly useful for the observation of the phonon at the low scattering angle. In fact, we have confirmed in our experiment that the phonon oscillation is observable even in the scattering angle of 0.1°. In the phase transition phenomena, this offers an ideal tool for the investigation of the soft phonon modes, because in the ordinary second-order, displacive-type phase transition, the phonon mode softens toward $|\mathbf{q}| = 0$.

From the viewpoints of the frequency region, the present method is suitable for the observation of the low-frequency region. Contrary to this, the highest observable frequency is limited by the time width of the exciting pulse. In our experiment, the upper limit is about 3 GHz. This is in contrast to the ordinary light scattering experiment where the resolution of the monochromator determines its lowest-frequency limit. However, to increase the upper frequency limit of the present spectroscopy is not so difficult owing to the recent development of femtosecond laser technique. In fact, Yan *et al.*[23] and recently Weiner *et al.*[24] performed the excitation of optical phonons up to several THz. Higher-frequency region may be covered by stimulated Raman scattering using two pulsed lasers. Hence this spectroscopy may cover the whole energy region for phonons of interest. Since the material response time near the phase transition temperature rapidly changes over many orders of magnitude, the use of this spectroscopy for the study on the phase transition phenomena must become a powerful tool.

The new features of our ISBS phonon spectroscopy, which allow further exploitation of the advantages demonstrated earlier, are the following.

(1) The use of cw probing coupled with a digital oscilloscope allows a real-time time-domain measurement which permits an extremely high resolution in frequency regime and also a very short acquisition time.

(2) The cw probing also allows us to combine a frequency-domain measurement with the ISBS. This offers a frequency-resolved phonon spectrum for the coherent phonons generated impulsively. The use of the frequency-domain measurement is promising particularly for the weak signals otherwise buried under unwanted background due to the scattered probe light.

(3) The use of a spatially translated probe beam allows us to observe directly the propagation of acoustic wave packets generated by the ISBS. The traveling wave packet is clearly observed by the time delay and nonoscillating signals in the time-domain measurement and by the asymmetric Brillouin doublets in the frequency-domain measurement. This method may be applicable to observe phonons with a small dumping rate or with a unusual dispersion relation.

(4) The time- and frequency-domain measurements also allow the clear discriminations of the resonance and nonresonance conditions for the phonon excitation by a pulse train. The resonance excitation of phonons is especially promising for the selective excitation of very weak phonons.

These features are of great advantage for the study on the low-frequency and small-wave-number phonon spectroscopy. Many applications may be expected[25] such as the observation of soft phonon mode in the phase transition, the slow relaxation processes concerning glasses, polymers, liquid crystals, and so on. However, to utilize generated phonons more actively, the selective excitation of phonons attracts much interest.[1,12,24] To do this experimentally, it is possible to use the mode-locked pulse train as in the present experiment or, more simply, to use intensity-modulated broad pulse as a light source. In the higher frequency region, Weiner *et al.*[24] attempted to produce the pulse train in THz region using femtosecond pulse and phase modulation technique. When these pulse trains are combined with a Pockels cell, a definite number of the pulses with almost equal intensities may be available. Then the forced oscillation of the phonon by this pulse train and the observation of the resulting free oscillation with damping offer the direct observation of the dynamics for the specified phonon. Further application along this course is highly desirable.

ACKNOWLEDGMENTS

This work is supported by a Grant-in-Aid for Scientific Research from the Ministry of Education, Science and Culture of Japan (No. 03452025), by Shimadzu Science Foundation, and also by Yamada Science Foundation.

[1] K. A. Nelson and M. D. Fayer, J. Chem. Phys. **72**, 5202 (1980); K. A. Nelson, D. R. Lutz, M. D. Fayer, and L. Madison, Phys. Rev. B **24**, 3261 (1981); K. A. Nelson, R. J. D. Miller, and M. D. Fayer, J. Appl. Phys. **53**, 1144 (1982); M. D. Fayer, Ann. Rev. Phys. Chem. **33**, 63 (1982).
[2] Y.-X. Yan, L.-T. Cheng, and K. A. Nelson, J. Chem. Phys. **88**, 6477 (1988).
[3] S. M. Silence, A. R. Duggal, L. Dhar, and K. A. Nelson, J. Chem. Phys. **96**, 5448 (1992).
[4] L.-T. Cheng, Y.-X. Yan, and K. A. Nelson, J. Chem. Phys. **91**, 6052 (1989); A. R. Duggal and K. A. Nelson, *ibid.* **94**, 7677 (1991).
[5] S. D. Silvestri, J. G. Fujimoto, E. P. Ippen, E. B. Gamble, Jr., L. R. Williams, and K. A. Nelson, Chem. Phys. Lett. **116**, 146 (1985).
[6] M. M. Robinson, Y.-X. Yan, E. B. Gamble, Jr., L. R. Williams, J. S. Meth, and K. A. Nelson, Chem. Phys. Lett. **112**, 491 (1984); M. Robinson Farrar, L.-T. Cheng, Y.-X. Yan, and K. A. Nelson, IEEE Quantum Electron. **QE-22**, 1453 (1986).
[7] L.-T. Cheng and K. A. Nelson, Phys. Rev. B **37**, 3603 (1988).
[8] L.-T. Cheng and K. A. Nelson, Phys. Rev. B **39**, 9437 (1989).
[9] T. P. Dougherty, G. P. Wiederrecht, and K. A. Nelson, Ferroelectrics **120**, 79 (1991).

[10] A. R. Duggal, J. A. Rogers, and K. A. Nelson, Appl. Phys. Lett. **60**, 692 (1992); J. Appl. Phys. **72**, 2823 (1992).
[11] S. Kinoshita and T. Yagi, Solid State Phys. (Japanese) **28**, 273 (1993).
[12] D. Pohl and W. Kaiser, Phys. Rev. B **1**, 31 (1970).
[13] S. Kinoshita, W. Tsurumaki, Y. Shimada, and T. Yagi, J. Opt. Soc. Am. B **10**, 1017 (1993).
[14] H. Eichler and H. Stahl, J. Appl. Phys. **44**, 3429 (1973).
[15] G. Cambon, M. Rouzeyre, and G. Simon, Appl. Phys. Lett. **18**, 295 (1971).
[16] J. W. Wagner, J. B. Deaton, Jr., and J. B. Spicer, Appl. Opt. **27**, 4696 (1988).
[17] J. B. Deaton, Jr., A. D. W. McKie, J. B. Spicer, and J. W. Wagner, Appl. Phys. Lett. **56**, 2390 (1990).
[18] G. Eyring and M. D. Fayer, J. Chem. Phys. **81**, 4314 (1984).
[19] F. W. Deeg and M. D. Fayer, J. Chem. Phys. **91**, 2269 (1989); Chem. Phys. Lett. **167**, 527 (1990).
[20] G. K. L. Wong and Y. R. Shen, Phys. Rev. A **10**, 1277 (1974).
[21] Y.-X. Yan and K. A. Nelson, J. Chem. Phys. **87**, 6257, 6270 (1987).
[22] H. Z. Cummins and R. W. Gammon, J. Chem. Phys. **44**, 2785 (1966).
[23] Y.-X. Yan, E. B. Gamble, Jr., and K. A. Nelson, J. Chem. Phys. **83**, 5391 (1985).
[24] A. M. Weiner, D. E. Leaird, G. P. Wiederrecht, and K. A. Nelson, J. Opt. Soc. Am. B **8**, 1264 (1991).
[25] L.-T. Cheng and K. A. Nelson, Ferroelectrics **117**, 1 (1991); J. Toulouse, M. I. Bell, K. A. Nelson, and N. Dalal, Ferroelectrics **120**, 1 (1991).